AIAA JOURNAL
Vol. 36, No. 6, June 1998

Numerical Simulation of Three-Dimensional Trailing Vortex Evolution in Stratified Fluid

Robert E. Robins* and Donald P. Delisi†
Northwest Research Associates, Inc., Bellevue, Washington 98009-3027

Numerical solutions to the Navier–Stokes equations that depict the evolution of a trailing vortex pair descending in stratified, incompressible fluid are presented. Both three-dimensional and two-dimensional results are shown for the Froude numbers 1, 2, 4, and 8 and infinity. For three and two dimensions, the results indicate that stratification, through generation of countersign vorticity, causes the separation between the vortices to decrease and, through buoyancy forces, suppresses the vertical migration of the vortices. In three dimensions, Crow instability causes the vortices eventually to link and to form rings when the Froude number is greater than or equal to 4, and the rate at which the linking and ring formation occur is greater for higher stratification (lower Froude number). The formation of rings is suppressed, however, for stratification so high that the Froude number is less than or equal to 2.

Nomenclature

b_0 = initial distance between vortices
Fr = Froude number, V_0/Nb_0
g = gravitational acceleration
H = nondimensional descent distance, h/b_0
h = dimensional descent distance
m = axial wave number of perturbation
N = Brunt–Väsäilä frequency of stratified fluid, $N^2 = -(g/\rho_0)\,\mathrm{d}\rho/\mathrm{d}z$
Re = Γ_0/ν
r_0 = radius of vortex cores
T = nondimensional time, t/T_0
T_0 = time for vortices to descend b_0, b_0/V_0
t = dimensional time
u = axial flow velocity component
V_0 = initial descent speed of vortices, $\Gamma_0/2\pi b_0$
v = cross-axial flow velocity component
w = vertical flow velocity component
x = axial coordinate
y = cross-axial coordinate
z = vertical coordinate
Γ_0 = initial circulation magnitude about each vortex, $2\pi b_0 V_0$
δ = initial peak-to-peak amplitude of sinusoidal instability
ε = measure of numerical accuracy
$\theta(z)$ = ambient potential temperature profile
θ_0 = representative value of ambient potential temperature
ν = kinematic viscosity
$\rho(z)$ = ambient density profile
ρ_0 = representative value of ambient density

I. Introduction

SINCE 1970, the two-dimensional behavior of a trailing wake vortex pair in stratified fluid has been the subject of numerous studies. To cite a few of these, a numerical approach was taken by Hill,[1] Hecht et al.,[2,3] Sarpkaya and Johnson,[4] Robins and Delisi,[5] and Spalart,[6] and analytical work was reported by Scorer and Davenport,[7] Saffman,[8] and Crow.[9] These studies resulted in two distinctly different views of trailing vortex evolution in stratified fluids. Spalart's study supported the conclusions of Scorer and Davenport and of Crow, that the effect of stratification is to decrease the separation between the vortices and cause an acceleration in their vertical motion. Their conclusion was that vortices in a stratified fluid could migrate farther than identical vortices in a nonstratified fluid. The other studies led to the conclusion that stratification causes a deceleration in the vertical motion of the vortices and, hence, a decreased vertical migration compared with that in a nonstratified fluid. Available observations such as the two-dimensional laboratory studies of Tomassian,[10] the three-dimensional laboratory studies of Sarpkaya[11] and Neuhart et al.,[12] the light aircraft data reported by Tombach,[13] and the widely used heuristic two-dimensional theory of Greene,[14] all supported the latter (deceleration) conclusion. This duality in understanding was discussed by Widnall.[15]

Recently, we have performed numerical simulations of three-dimensional trailing vortex evolution in stratified fluids that show that stratification initially causes the vortices to move together and that buoyancy effects, in combination with three-dimensional effects such as Crow instability and linking, can prevent the sustained vertical acceleration of the vortices. Our calculations were performed for vortex Froude numbers of 1, 2, 4, and 8, which, for a B-747 in cruise configuration, correspond to Brunt–Väisälä frequencies of approximately 0.04, 0.02, 0.01, and 0.005 rad/s, respectively. For our calculations, $\mathrm{d}\rho/\mathrm{d}z$ (and thus N) is chosen to be constant with height. Note, as is evident from recent measurements,[16] that values of N up to about 0.025 rad/s (corresponding to a potential temperature lapse rate of 2°C per 100 m) are commonly observed in the atmosphere. Based on evidence presented by Spalart,[17] we consider a value of 0.04 to be a reasonable upper limit.

In previous work,[18] we showed results from calculations without stratification that agreed with and extended the perturbation analysis of Crow.[19] This agreement validated our code, and an updated (to include stratification) version of that code has been used to produce the results presented herein. We will infer from the results presented later that stratification accelerates the linking of three-dimensional trailing vortices and suppresses their vertical migration. These results for three-dimensional trailing vortex evolution in a stratified fluid clarify and extend what has been learned from two-dimensional calculations.

In the following sections, we review our numerical approach (Sec. II), present results (Sec. III), and draw conclusions (Sec. IV).

II. Numerical Approach

As in Ref. 18, we solve the three-dimensional Navier–Stokes equations of motion. In this study, we include the effects of buoyancy. To solve the equations of motion, we use highly accurate finite difference approximations for the spatial discretizations and ensure incompressibility by using a two-phase projection method to evolve the solution forward in time. A second-order Adams–Bashforth method is used for the advection phase of the projection method, and a fast Poisson solver is used for the projection phase. Horizontal derivatives are computed using fast Fourier transforms,

Received March 1, 1996; revision received Jan. 9, 1998; accepted for publication Feb. 11, 1998.

*Research Scientist, P.O. Box 3027. Member AIAA.
†Senior Research Scientist, P.O. Box 3027. Member AIAA.

and a sixth-order compact scheme is used for vertical derivatives. Horizontal boundary conditions are periodic, and "no surface" conditions (vertical derivatives equal zero) are imposed at the top and bottom of the computational domain. The two-thirds rule is used to avoid aliasing errors, and Fourier and compact low-pass filters are used in the horizontal and vertical directions, respectively, to control the buildup of small-scale energy. Both the compact derivative and the compact filter schemes are based on the work of Lele.[20] The computational domain is doubled in width or translated vertically when migrating vortices approach the cross-axial or vertical boundaries, respectively.

All calculations presented in the current study were initialized by vortices formed from a superposition of many component vortices, each having a different perturbation wavelength and phase. Each component is a nearly parallel pair of counter-rotating vortices, with axes perturbed sinusoidally from parallel. We choose the total peak-to-peak amplitude of each component to be $0.02b_0$ and set the core radii of the vortices to be $0.16b_0$. The wavelength of each component depends on its wave number and the axial extent of the computational domain. The energies of the various component vortex pairs are chosen to scale as $m^{-5/3}$, and the relative phases are randomly selected. The circulations of the component vortices are normalized so that the circulation for the composite trailing vortices is the same as it would be if all of the circulation were assigned to a single-component vortex pair. Because of the random phases, the peak-to-peak perturbation amplitude of the composite vortices is only $0.008b_0$. Further details are available in Ref. 18.

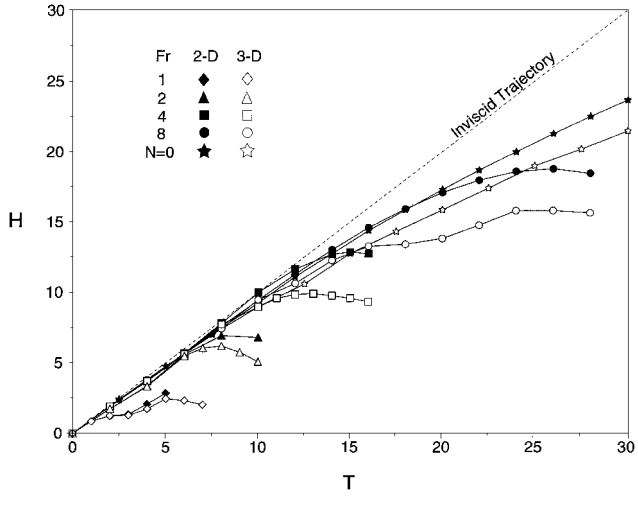

Fig. 1 Normalized vertical migration distance H vs normalized time T for two-dimensional and three-dimensional vortices for Fr = 1, 2, 4, 8, and infinity (N = 0). The dashed line represents $H = T$.

For the calculations presented herein, the vortex Reynolds number was chosen sufficiently large that viscous diffusion in the vortex cores was minimal. At the same time, the Reynolds number was chosen to be small enough to allow the time step required for a stable calculation to be sufficiently large that calculations could be completed in a reasonable amount of time. The value of the Reynolds number that we used was approximately 3×10^3, and the size of the time step was such that there were between 400 and 500 steps per T_0.

The numerical accuracy of all computational results was monitored by calculating the quantity $\varepsilon = \mathrm{SQRT}(\langle \mathrm{DIV}^2 \rangle / \langle \mathrm{GRADSQ} \rangle)$, where $\mathrm{DIV} = \partial u/\partial x + \partial v/\partial y + \partial w/\partial z$, $\mathrm{GRADSQ} = (\partial u/\partial x)^2 + (\partial v/\partial y)^2 + (\partial w/\partial z)^2$, and $\langle\rangle$ indicates an average over the computational domain. The quantity ε is a measure of the incompressibility of computed flows; the value of ε for an incompressible flow should be zero. Our criterion for a calculation to be of acceptable accuracy was that the value of ε at the conclusion of the calculation be less than 0.01. This criterion was satisfied for all computed flows presented next.

III. Results

We first present results for $Fr = 1, 2, 4, 8$, and infinity ($N = 0$), which show the effect of stratification on the vertical migration of trailing vortices. We will then examine these cases in more detail and discuss the importance of three-dimensional effects.

Figure 1 shows H vs T for $Fr = 1, 2, 4, 8$, and infinity, where H is the vertical descent of the vortices normalized by b_0 and T is time normalized by T_0. The open symbols denote three-dimensional results. We also ran the code with single-component, unperturbed initial vortices having a limited axial extent equal to $0.625b_0$. These results are labeled 2-D and are shown by the solid symbols in Fig. 1. The following discussion pertains to the three-dimensional results except where the two-dimensional results are explicitly mentioned. The axial extent of the computational domain in each case is $20b_0$, and the axial wave numbers of the component vortices range from 2 to 16. The cross-axial extent is $10b_0$, and the vertical extent varies, being larger for higher Froude numbers. The numbers of grid points in each case are 256 and 128 for the axial and cross-axial directions, and the vertical grid spacing is chosen to approximately match the resolution in the horizontal directions. Because the evolution of the vortices is three dimensional, the value of H for each T varies along the axial extent of the computational domain. The H values plotted in Fig. 1 are the average of the maximum and minimum heights of the vortex cores.

Figure 1 shows, for $Fr = 1, 2, 4$, and 8, that three-dimensional and two-dimensional vortices migrate vertically and eventually reach a point of maximum migration. Buoyancy forces arrest the vertical motion of the vortices and cause them to lose their identity after the last point plotted for these cases. For the $N = 0$ case, the vortices continue to migrate as vortex rings beyond the last point plotted. It is clear from Fig. 1 that, as stratification increases (Froude number decreases), the maximum vertical migration of the vortices decreases.

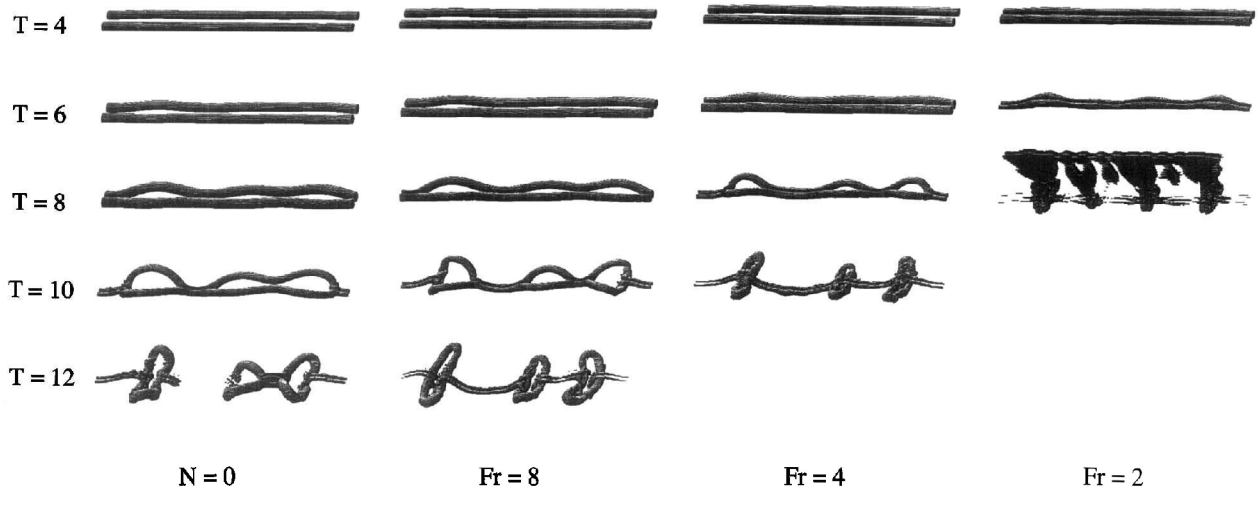

Fig. 2 Time variation of vorticity magnitude surfaces for Fr = 8, 4, 2, and infinity (N = 0). Vorticity magnitude at the visualized surfaces is 20% of the maximum value at the vortex cores.

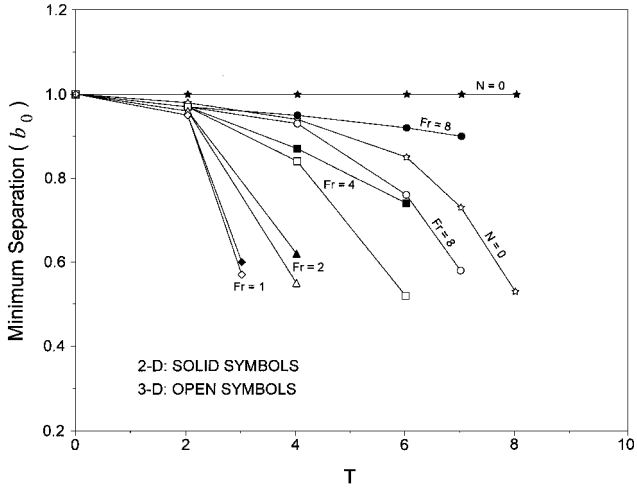

Fig. 3 Minimum vortex separation, normalized by the initial separation, vs normalized time for two-dimensional and three-dimensional vortices for Fr = 1, 2, 4, 8, and infinity (N = 0).

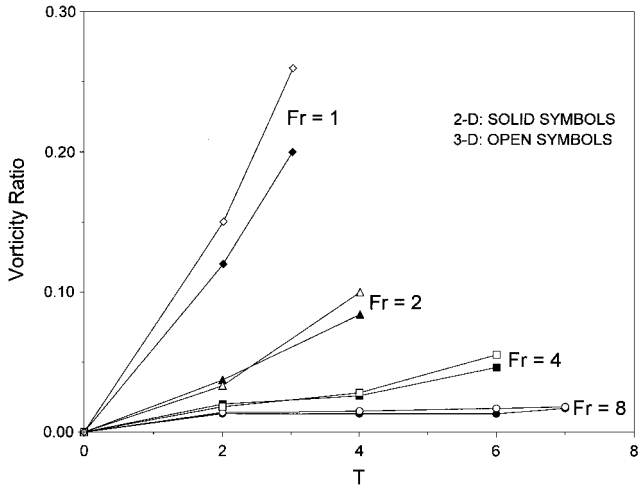

Fig. 4 Ratio of maximum generated countersign vorticity to maximum core vorticity vs normalized time for two-dimensional and three-dimensional vortices for Fr = 1, 2, 4, and 8.

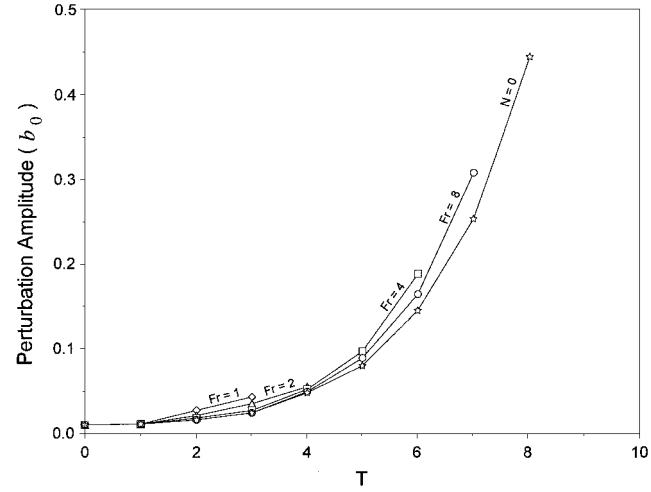

Fig. 5 Normalized peak-to-peak perturbation amplitude vs normalized time for Fr = 1, 2, 4, 8, and infinity (N = 0).

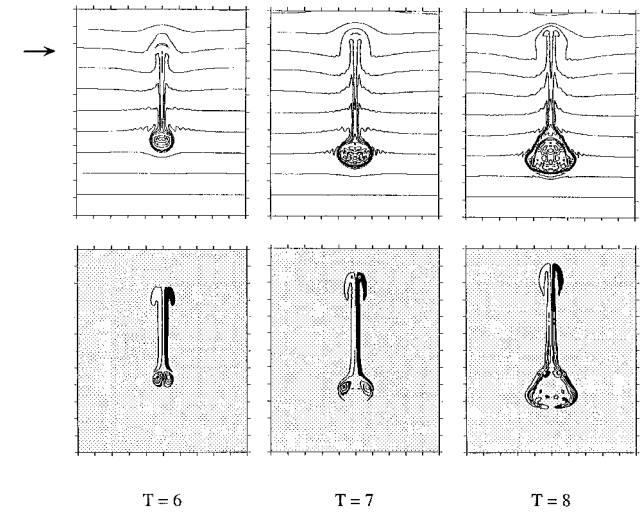

Fig. 6 Contour plots at T = 6, 7, and 8, of density (top) and vorticity (bottom) in the cross-axial vertical plane located at the axial position of the leftmost puff appearing in Fig. 2 for Fr = 2 at T = 8. The horizontal arrow indicates the starting height of the vortices. The distance between tick marks on the contour plots represents b_0.

Note that the two-dimensional vortices always migrate farther than the three-dimensional vortices for the same Froude number. This larger suppression of vertical migration for three-dimensional vortices than for two-dimensional vortices occurs even for the strongest stratifications (Froude numbers of 1 and 2).

The effect of stratification on the three-dimensional evolution of trailing vortices can be qualitatively seen from Fig. 2, which shows the time variation of surfaces of constant vorticity magnitude for $N = 0$ and $Fr = 8$, 4, and 2. Vorticity magnitude at the visualized surfaces is 20% of the maximum value at the vortex cores. In each case, the first result shown is for $T = 4$. Subsequent results are shown every two time units until the vortices link and form rings. For $Fr = 2$, the stratification is strong enough to suppress the formation of rings, causing instead the development of structures that we call puffs. It is clear that increasing stratification (decreasing Froude number) accelerates the vortices' linking and the formation of rings. The case $Fr = 1$ is not shown because, by $T = 4$, buoyancy effects have essentially halted the vortices' migration and evolution. Further discussion of the $Fr = 1$ case appears at the end of this section.

By comparing Fig. 2 with Fig. 1 for a particular Froude number, we can see that the time at which rings or puffs form (for $Fr \geq 2$) corresponds to the time when the descent of the three-dimensional vortices starts to lag the descent of the two-dimensional vortices. For example, we see from Fig. 2 that rings are formed by $T = 12$ for $Fr = 8$, and Fig. 1 shows the three-dimensional H vs T plot for $Fr = 8$ falling below the two-dimensional plot for $Fr = 8$ by $T = 14$. Similar comparisons can be made for the other $Fr \geq 2$.

Thus, it can be concluded that, once the three-dimensional rings are formed, they travel vertically more slowly than the two-dimensional vortices for the same Froude number.

The acceleration of linking for increased stratification observed in Fig. 2 is quantified in Fig. 3. Here we show minimum vortex separation vs time, until near linking, for the vortices in Fig. 2. The case $Fr = 1$ is included on the plot, as well as separations obtained from the two-dimensional simulations. It is clear that increased stratification results in a more rapid reduction in the minimum vortex spacing. It is also evident that, for a fixed Froude number, the reduction is greater for three dimensions than for two dimensions and that the difference between the three-dimensional and two-dimensional reduction increases as time increases.

Two mechanisms are contributing to these effects. It is known from two-dimensional studies that countersign vorticity generated during the vortices' evolution will force the vortices closer together, e.g., see Refs. 5 and 6. We also know that Crow instability will perturb the vortices and move portions of the vortices closer together. In Figs. 4 and 5, we show how these mechanisms are affected by changes in stratification.

In Fig. 4, we show the effect of stratification on the relative strength of the generated countersign vorticity for two-dimensional and three-dimensional flows. We represent the relative strength of countersign vorticity as the ratio of maximum generated countersign vorticity to maximum vorticity in the vortex cores. Figure 4 shows

plots of this ratio vs time, until the vortices link, for two-dimensional and three-dimensional simulations. For the three-dimensional case, the ratio is computed in a vertical plane located at the axial position where the vortices have moved closest to each other. We see that the ratio increases for increasing stratification (decreasing Froude number) and that it tends to be somewhat greater for three dimensions than for two dimensions. Clearly, the stratification effect is stronger than the three-dimensional effect.

In Fig. 5, we show the effect of stratification on perturbation growth in three-dimensional flows. Figure 5 shows peak-to-peak perturbation amplitude vs time, until the vortices link, for the Froude numbers 1, 2, 4, 8, and infinity. The amplitude is evaluated as the maximum horizontal peak-to-peak amplitude for the core of a single vortex. We see that the perturbation amplitude increases strongly with time and that the amplitude growth is only modestly enhanced by increasing stratification.

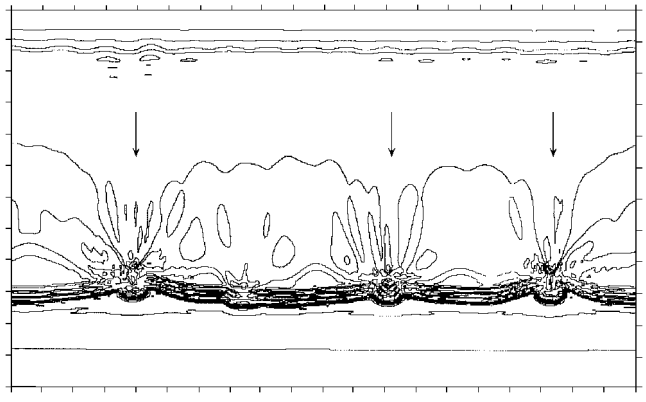

Fig. 7 Contour plot of density in a vertical plane midway between the cores of the vortices at $T = 7$ for the $Fr = 2$ case. The vertical arrows indicate the axial locations where puffs have started to form. The distance between tick marks on the contour plots represents b_0.

Going back to Fig. 3, we see that for times less than or equal to $T = 4$ the stratification effect dominates the three-dimensional effect, but for times greater than or equal to $T = 6$, the three-dimensional effect becomes more significant. If we compare Figs. 4 and 5 with Fig. 3, we see that the dominance of stratification effects shown in Fig. 4 for $T \leq 4$ is well correlated with the dominant stratification effects for early times in Fig. 3. Also, the dominance of three-dimensional effects in Fig. 5 for later times (larger perturbation amplitude) is well correlated with the three-dimensional vs two-dimensional differences seen for later times in Fig. 3. We thus infer that stratification, manifested through countersign vorticity generation, governs the initial three-dimensional vortex evolution and that perturbation growth is the dominant factor in the later stages of three-dimensional vortex evolution.

Returning to Fig. 2, we note that vortex evolution for $N = 0$ and $Fr = 8$ and 4 is qualitatively similar in that the vortices link and rings are formed. For $Fr = 2$, however, ring formation is suppressed and puffs are formed. It turns out, as we will explain, that axial density gradients play an important role in this phenomenon.

We focus on times $T = 6$, 7, and 8 for $Fr = 2$. We first refer back to Fig. 2, where we see at $T = 6$ that the vortices for $Fr = 2$ are about to link. Their appearance is qualitatively similar to the vortices at $T = 8$ for $Fr = 4$ and 8 and to the vortices at $T = 10$ for $N = 0$, all of which are also about to link. Note, however, that the perturbation amplitudes in the $Fr = 2$ case are smaller than the perturbation amplitudes for the other cases at the times just mentioned.

At $T = 8$ for $Fr = 2$ in Fig. 2, we see vertical vorticity structures above the linked regions, connected to cross-axially extruded, axially compressed puffs. Details for one of these complex regions are shown in Fig. 6. Here we show contour plots at $T = 6$, 7, and 8 of density (top) and axial vorticity (bottom) in the cross-axial vertical plane that is located at the axial position of the leftmost puff for $Fr = 2$ at $T = 8$ in Fig. 2. The horizontal arrow in Fig. 6 shows the original generation level of the vortices. Figure 6 shows that light fluid has been entrained into bubbles and carried downward by the vortices. Buoyancy forces act to return the light fluid to its

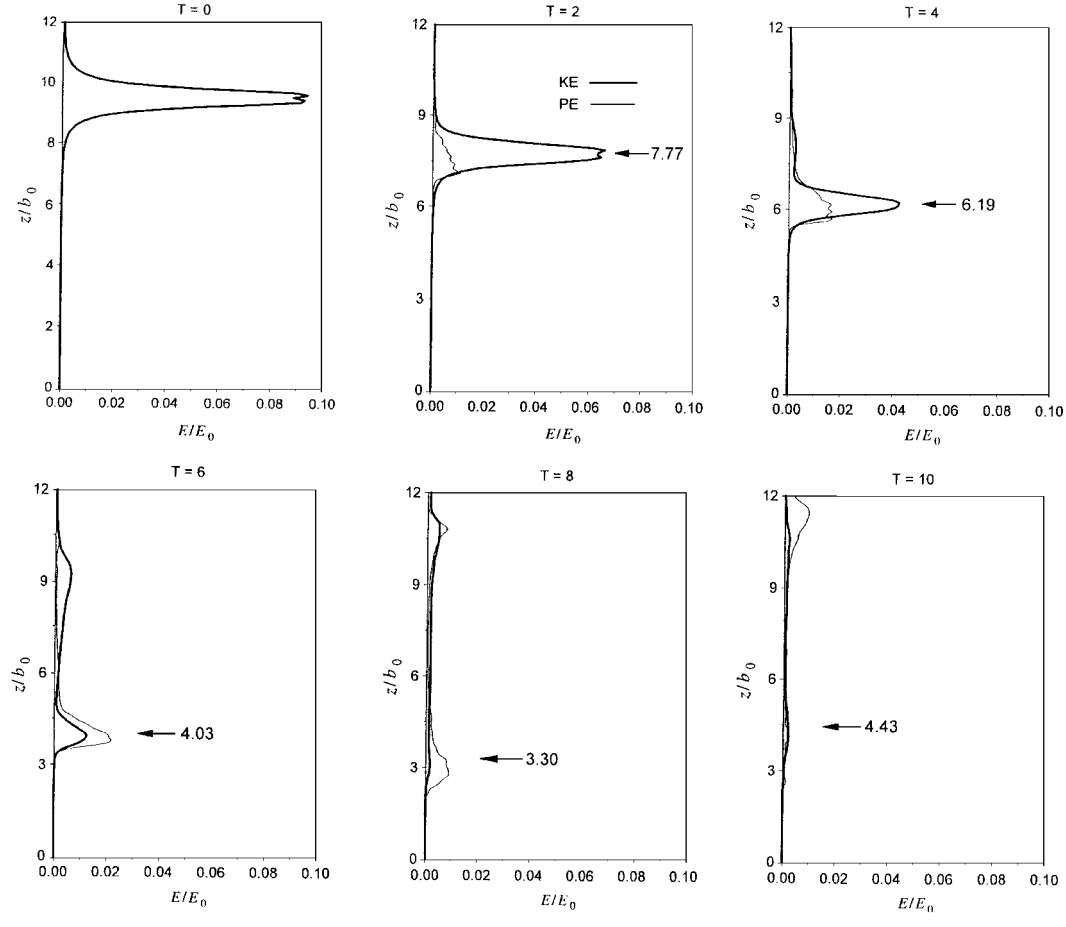

Fig. 8 Vertical profiles of horizontally averaged kinetic energy (KE) and potential energy (PE) for $Fr = 2$ at normalized times $T = 0$, 2, 4, 6, 8, and 10. The arrows indicate vertical positions of the vortices based on data from Fig. 1.

original level, but Figs. 2 and 6 show that, rather than rising, the fluid appears to move cross axially.

To explain this, we look at Fig. 7, which shows the density field in a vertical plane midway between the cores of the two vortices at $T = 7$ for the $Fr = 2$ case. Downward-pointing arrows indicate the axial locations where puffs have started to form. The leftmost arrow is at the location of Fig. 6. On either side of the arrows, it can be seen that there are density gradients pointing toward the axial locations of the forming puffs but above the forming puffs themselves. These oppositely directed, axial density gradients prevent the light fluid, which has been carried downward, from returning to its original position. Instead, circulations are created that steer the rising fluid in a cross-axial direction, giving rise to the structures seen in Figs. 2 and 6.

Another view of the $Fr = 2$ case appears in Fig. 8, which shows vertical profiles of horizontally averaged kinetic energy (KE) and potential energy (PE) at $T = 0$, 2, 4, 6, 8, and 10 for the three-dimensional $Fr = 2$ simulation. The arrow in each plot denotes the vertical position of the descending vortices in correspondence with the three-dimensional $Fr = 2$ case in Fig. 1. The z/b_0 values shown at each arrow are obtained by subtracting the appropriate H value in Fig. 1 from the starting height $z/b_0 = 9.5$. Note that by $T = 8$ there is a peak in PE but very little KE at the level at which the puffs have formed. This means that, although we observe structure in the puff regions shown in Fig. 6 for $T = 8$, there is very little kinetic energy at the depth of the puffs. By $T = 10$, there is almost no energy associated with the remaining lower-level vorticity.

One other noteworthy feature in Fig. 7 is the small-scale oscillation (wavelength on the order of b_0) in the density field at the top of the plot. This oscillation is indicative of a small-scale instability that becomes more pronounced as stratification increases. (See Ref. 21, where laboratory observations and numerical simulations of this instability are reported for $Fr = 1$.)

Note that the $Fr = 1$ case is quite different from the other cases we have presented. Because the buoyancy timescale (typically π/N) for $Fr = 1$ is much shorter than the linking timescale (typically $6b_0/V_0 = 6/N$), linking never occurs. Thus, the puffs observed in the $Fr = 2$ case are not observed when $Fr = 1$. Instead the light fluid that has been carried downward returns to its original level. In addition, small-scale instabilities (referred to earlier) disrupt any remaining axial coherence.

IV. Concluding Remarks

Our numerical simulations have shown that stratification effects on three-dimensional trailing vortex evolution bear some resemblance to the two-dimensional case but also show important differences. As in the two-dimensional case, the vortices descend, countersign vorticity is generated, and the minimum separation between the vortices is decreased. However, in the three-dimensional case, perturbation growth due to Crow instability combines with countersign vorticity generation to accelerate the coming together of other portions of the vortices.

We have also shown that the three-dimensional simulations exhibit phenomena that do not exist in two dimensions. For zero to weak to moderate stratification, three-dimensional vortices link and form rings, and for sufficiently strong stratification, axial gradients are formed that alter the buoyancy dynamics of the flow, resulting in the formation of three-dimensional structures that we have termed *puffs*. As stratification is increased in the three-dimensional case, we see an acceleration in linking and the formation of rings. This acceleration is caused initially by countersign vorticity effects and later by perturbation growth due to Crow instability. Indeed, the stratification and the Crow instability working together produce an effect significantly greater than the Crow instability on its own. We can see this in the three-dimensional simulations by noting that at $T = 6$ the difference in minimum separation (due to stratification and Crow instability) between the $N = 0$ and $Fr = 4$ cases is $>0.3b_0$ (see Fig. 3), whereas the difference in perturbation amplitude (which is due to Crow instability alone) for the same Froude numbers at the same time is $<0.05b_0$ (see Fig. 5). An important consequence of the formation of rings or puffs is that, once these structures are formed, the descent of the three-dimensional vertices lags the descent of the two-dimensional vertices for the same Froude number.

Finally, we mention that our previous results have shown that vortex linking will be accelerated by tighter vortex cores and larger initial perturbations, e.g., from strong ambient turbulence, and decelerated by broader cores and smaller initial perturbations. Thus, the phenomena that we have associated with certain Froude numbers could occur for somewhat lower or higher Froude numbers, depending on the details of the trailing vortex generation.

Acknowledgments

This work was performed under Naval Sea Systems Command Contract N00024-91-C-6312 and under Office of Naval Research Contract N00014-96-C-0060. The authors thank Robert J. Lynch and L. Patrick Purtell for their support and encouragement. All calculations were performed on a Cray C-90 at the U.S. Army Corps of Engineers Waterways Experiment Station.

References

[1]Hill, F. M., "A Numerical Study of the Descent of a Vortex Pair in a Stably Stratified Atmosphere," *Journal of Fluid Mechanics*, Vol. 71, Pt. 1, 1975, pp. 1–13.

[2]Hecht, A. M., Bilanin, A. J., Hirsch, J. E., and Snedeker, R. S., "Turbulent Vortices in Stratified Fluids," *AIAA Journal*, Vol. 18, No. 7, 1980, pp. 738–746.

[3]Hecht, A. M., Bilanin, A. J., and Hirsch, J. E., "Turbulent Trailing Vortices in Stratified Fluids," *AIAA Journal*, Vol. 19, No. 6, 1981, pp. 691–698.

[4]Sarpkaya, T., and Johnson, S. K., "Trailing Vortices in Stratified Fluids," U.S. Naval Postgraduate School, Rept. NPS-69-82-003, Monterey, CA, 1982.

[5]Robins, R. E., and Delisi, D. P., "Numerical Study of Vertical Shear and Stratification Effects on the Evolution of a Vortex Pair," *AIAA Journal*, Vol. 28, No. 4, 1990, pp. 661–669.

[6]Spalart, P. R., "On the Motion of Laminar Wing Wakes in a Stratified Fluid," *Journal of Fluid Mechanics*, Vol. 327, Nov. 1996, pp. 139–160.

[7]Scorer, R. S., and Davenport, L. J., "Contrails and Aircraft Downwash," *Journal of Fluid Mechanics*, Vol. 43, 1970, pp. 451–464.

[8]Saffman, P. G., "The Motion of a Vortex Pair in a Stratified Atmosphere," *Studies in Applied Mathematics*, Vol. 51, 1972, pp. 107–119.

[9]Crow, S. C., "Motion of a Vortex Pair in a Stratified Fluid," Poseidon Research, Rept. 1, Santa Monica, CA, May 1974.

[10]Tomassian, J. D., "The Motion of a Vortex Pair in a Stratified Medium," Ph.D. Dissertation in Engineering, Univ. of California, Los Angeles, 1979.

[11]Sarpkaya, T., "Trailing Vortices in Homogeneous and Density-Stratified Media," *Journal of Fluid Mechanics*, Vol. 136, Nov. 1983, pp. 85–109.

[12]Neuhart, D. H., Greene, G. C., Satran, D. R., and Holbrook, G. T., "Density Stratification Effects on Wake Vortex Decay," *Journal of Aircraft*, Vol. 23, No. 11, 1986, pp. 820–824.

[13]Tombach, I. H., "Observations of Atmospheric Effects on Vortex Wake Behavior," *Journal of Aircraft*, Vol. 10, No. 11, 1973, pp. 641–647.

[14]Greene, G. C., "An Approximate Model of Vortex Decay in the Atmosphere," *Journal of Aircraft*, Vol. 23, No. 7, 1986, pp. 566–573.

[15]Widnall, S. E., "The Structure and Dynamics of Vortex Filaments," *Annual Review of Fluid Mechanics*, Vol. 7, 1975, pp. 141–165.

[16]Campbell, S., Dasey, T., Freehart, R., Heinrichs, R., Matthews, M., and Perras, G., "Wake Vortex Field Measurements at Memphis, TN," AIAA Paper 96-0399, Jan. 1996.

[17]Spalart, P. R., "Airplane Trailing Vortices," *Annual Review of Fluid Mechanics*, Vol. 30, 1998, pp. 107–138.

[18]Robins, R. E., and Delisi, D. P., "Numerical Simulations of Three-Dimensional Trailing Vortex Evolution," *AIAA Journal*, Vol. 35, No. 9, 1997, pp. 1552–1555.

[19]Crow, S. C., "Stability Theory for a Pair of Trailing Vortices," *AIAA Journal*, Vol. 8, No. 12, 1970, pp. 2172–2179.

[20]Lele, S., "Compact Finite Difference Schemes with Spectral-Like Resolution," *Journal of Computational Physics*, Vol. 103, No. 1, 1992, pp. 16–42.

[21]Delisi, D., and Robins, R., "Small-Scale Instabilities in Trailing Wake Vortices in a Stratified Fluid," AIAA Paper 97-1784, July 1997.

F. W. Chambers
Associate Editor